Supporting Information

An oxazole-linked donor-acceptor covalent organic framework as an efficient electrocatalyst for lithium-sulfur batteries

*Xuanhe Hu[‡], Gengyuan Zhang[‡], Hongyuan Liang, Jiangtao Li, Hujing Zhou, Lai-Hon Chung and Jun He**

X. Hu, G. Zhang, H. Liang, J. Li, H. Zhou, L.-H Chung, J. He
School of Chemical Engineering and Light Industry, Guangdong University of Technology, Guangzhou 510006, P. R. China
X. Hu
Guangdong Provincial Key Laboratory of Functional Supramolecular, Coordination Materials and Applications, Jinan University, Guangzhou 510632, P. R. China
J. He
Guangdong Provincial Laboratory of Chemistry and Fine Chemical Engineering Jieyang Center, Jieyang 515200, P. R. China
E-mail: junhe@gdut.edu.cn
[‡]These authors contributed equally to this work

Experimental Section

Synthesis of BTT-DA

Briefly, a mixture of BTT (0.045 mmol) and phenylenediamine (DA, 0.067 mmol) was suspended in o-dichlorobenzene/n-butyl alcohol (1.125 mL/0.375 mL) with acetic acid as catalyst (6 M, 0.15 mL) in a Pyrex tube. After sonication for 10 min, the mixture was degassed three times by freeze-pump-thaw cycling. Subsequently, the Pyrex tube was heated at 120 ℃ for three days. The precipitate was centrifuged and extensively washed by THF for 72 h in a Soxhlet extractor. The powder was dried at 60 °C to obtain the final product which was a brown powder.

Visible adsorption tests

Li_2S_6 solution (0.5 mM) was firstly prepared by mixing sulfur and Li_2S (molar ratio of 5:1) and dissolved in a solvent of 3-dioxolane (DOL)/dimethoxymethane (DME) (v/v=1:1). 15 mg amount of BTT-DABD and BTT-DA was added to two glass bottles, respectively. Then, 2 mL Li_2S_6 solution was added dropwise to each glass bottle. Digital photographs were collected after resting for 12 h.

Symmetric cell and Li_2S nucleation experiments

Firstly, as-above slurry was casted onto Al foil current collector, which was then dried under vacuum. Two such electrodes were assembled into a CR2025 coin cell with Li_2S_6 electrolyte (0.5 M) and polypropylene separator. CV measurements of the symmetric cells were performed at 10 mV s^{-1} within a voltage range of −0.8-0.8 V. Nucleation of Li_2S on various COF surfaces was investigated in coin cells. The prepared electrode and lithium foil were used as work electrode and counter electrode, respectively. 20 μL of Li_2S_6 solution was applied as electrolyte. The assembled cell was first discharged 2.10 V at 0.112 mA and then held at 2.08 V.

Theoretical calculation

The theoretical calculations employed the Vienna Ab-inito Simulation Package (VASP).[1] The generalized gradient approximation (GGA) method with Perdew-Burke-Ernzerhof (PBE) functional is used to describe the exchange-correlation effects.[2] The energy cutoff of the plane-wave basis was set to 400 eV. The 1×1×1 k-

points were selected to sample the Brillouin zone integration. The binding energy (E_b) was calculated by

$$E_b = E_{total} - E_{Li2Sx} - E_{sub}$$

where E_{Li2Sx} and E_{total} are the calculated energies before and after the adsorption of Li_2S_x (x=1, 4, 6, 8) on the substrates, respectively. E_{sub} means the calculated energy of BTT-DA or BTT-DABD surface.

Supporting Figures

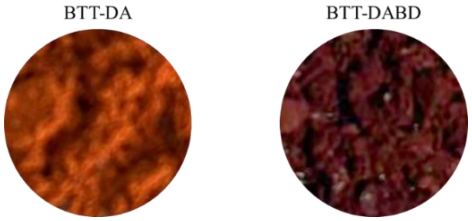

Figure S1. Photographs of BTT-DA and BTT-DABD.

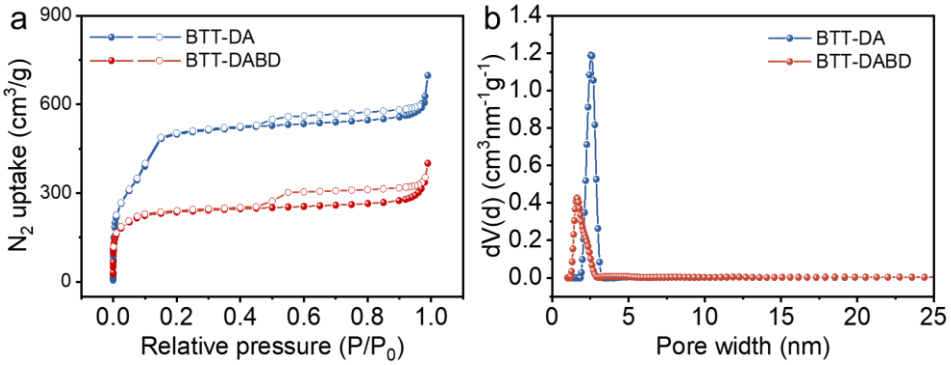

Figure S2. (a) N_2 adsorption–desorption isotherm and (b) pore size distribution profile of BTT-DABD and BTT-DA.

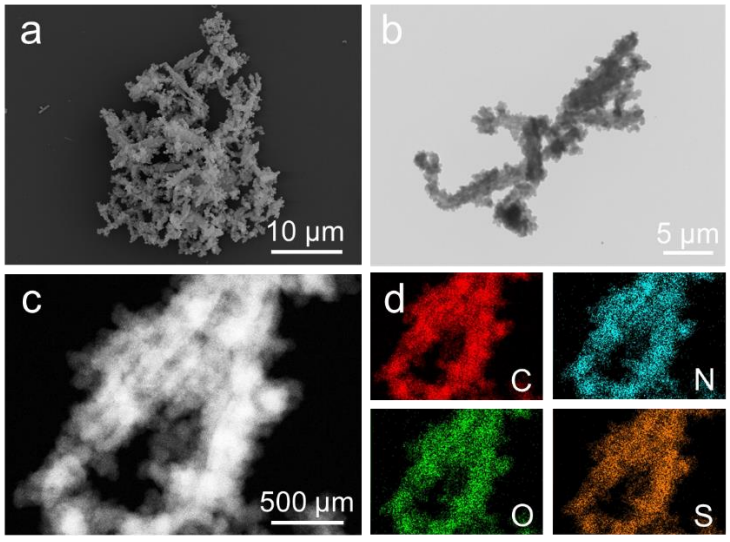

Figure S3. (a) SEM and (b) TEM images of BTT-DABD. (c, d) TEM and elecemtal mapping images of BTT-DABD.

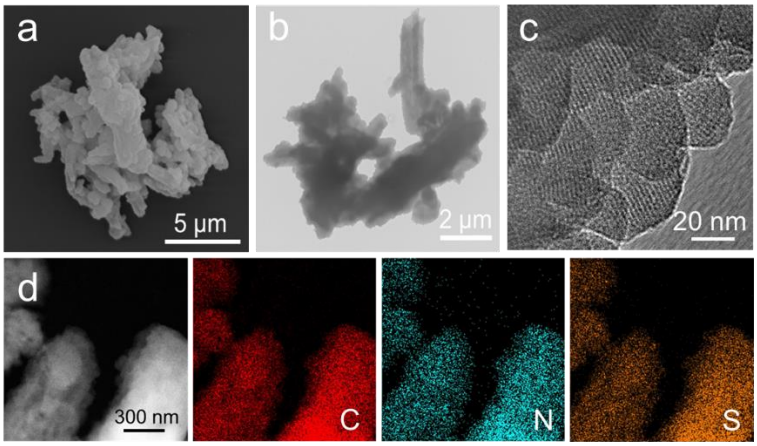

Figure S4. (a) SEM and (b, c) TEM images of BTT-DA. (d) TEM and elecemtal mapping images of BTT-DA.

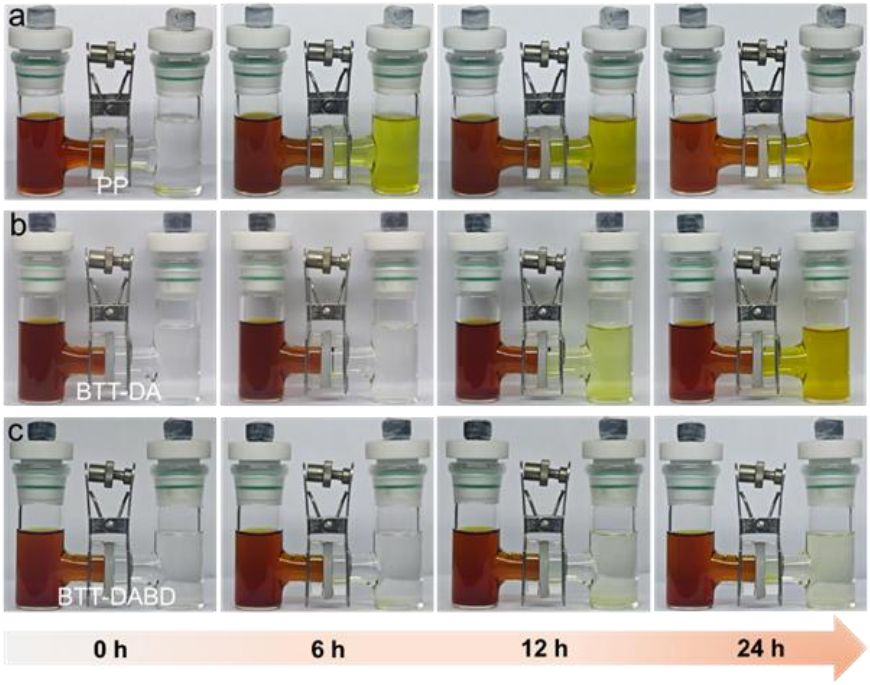

Figure S5. Visual image of Li_2S_6 H-cell diffusions tests with (a) PP, (b) BTT-DA and (c) BTT-DABD separators.

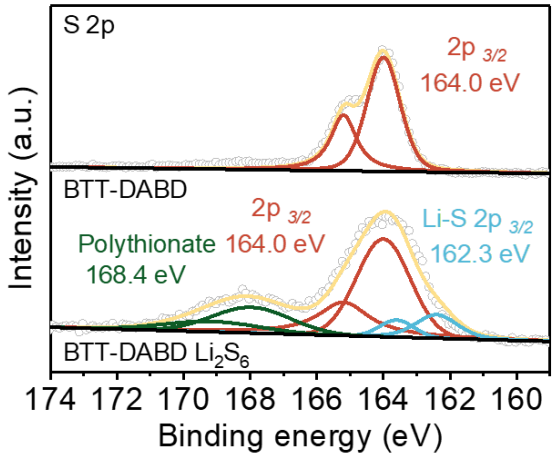

Figure S6. S 2*p* spectra of BTT-DABD before and after Li_2S_6 adsorption.

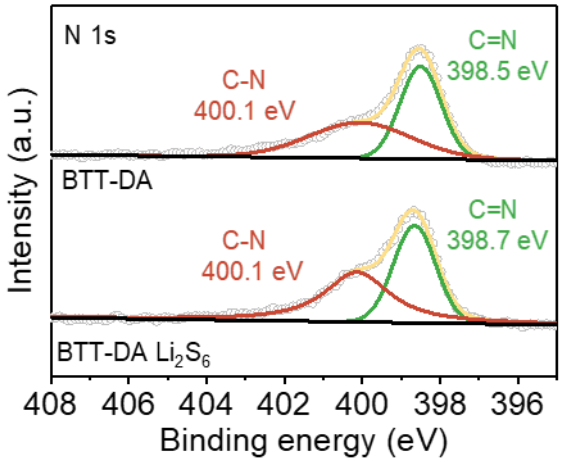

Figure S7. N 1s spectra of BTT-DA before and after Li_2S_6 adsorption.

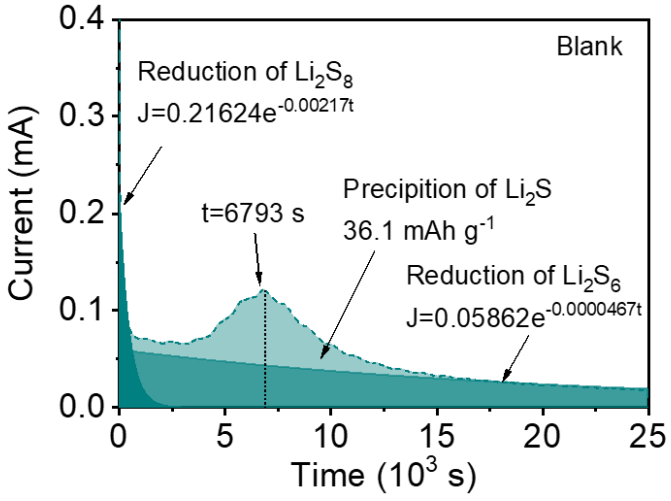

Figure S8. Potentiostatic discharge curves of the Li_2S_6 solution on blank electrodes.

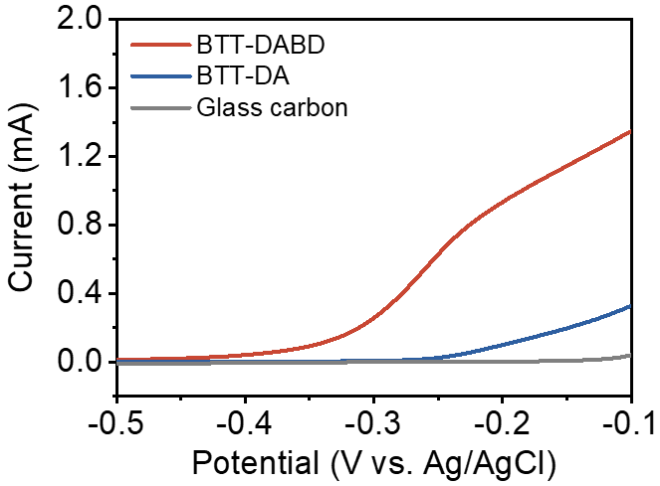

Figure S9. LSV curves of Li_2S oxidation on BTT-DABD, BTT-DA, and glass carbon electrodes.

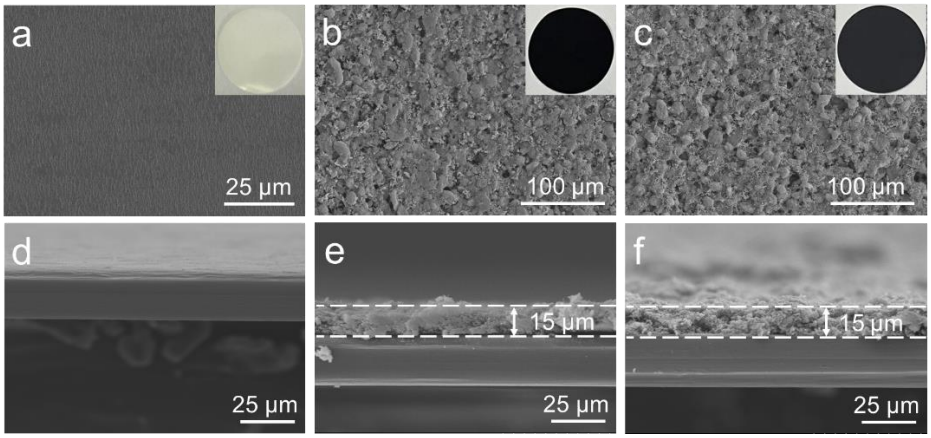

Figure S10. Top view and side view SEM images of (a, d) PP, (b, e) BTT-DA, and (c, f) BTT-DABD separators.

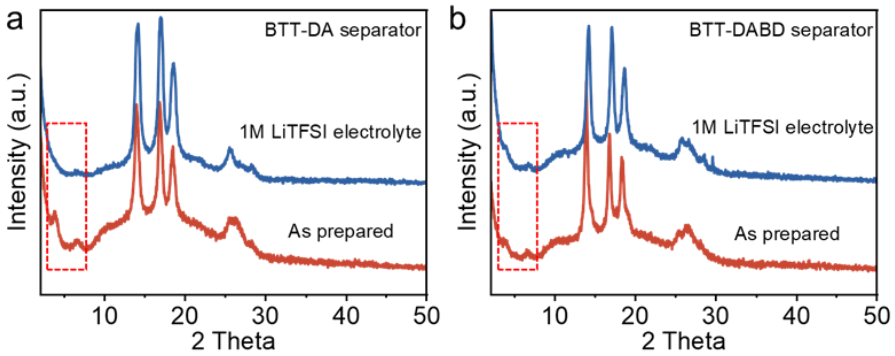

Figure S11. XRD patterns of (a) BTT-DA and (b) BTT-DABD separators before and after immersion in electrolyte for 12 h.

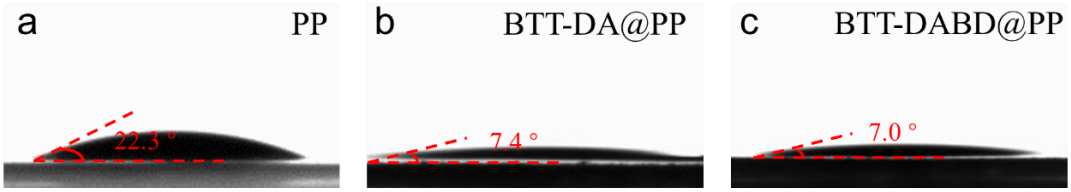

Figure S12. (a-c) Contact angle measurements of PP, BTT-DA and BTT-DABD separators.

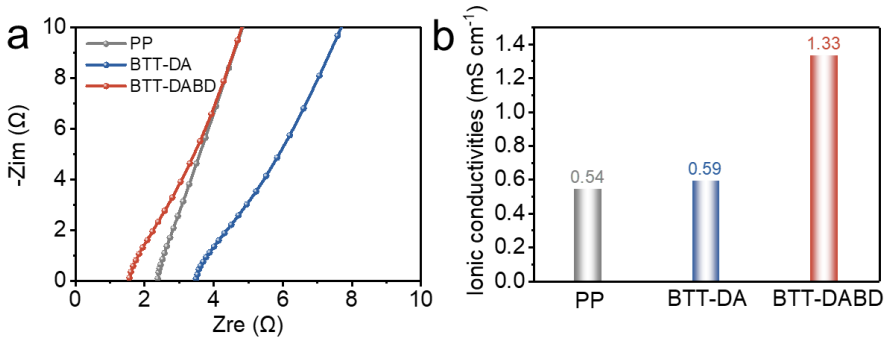

Figure S13. (a) EIS plots and (b) Ionic conductivities of different separators.

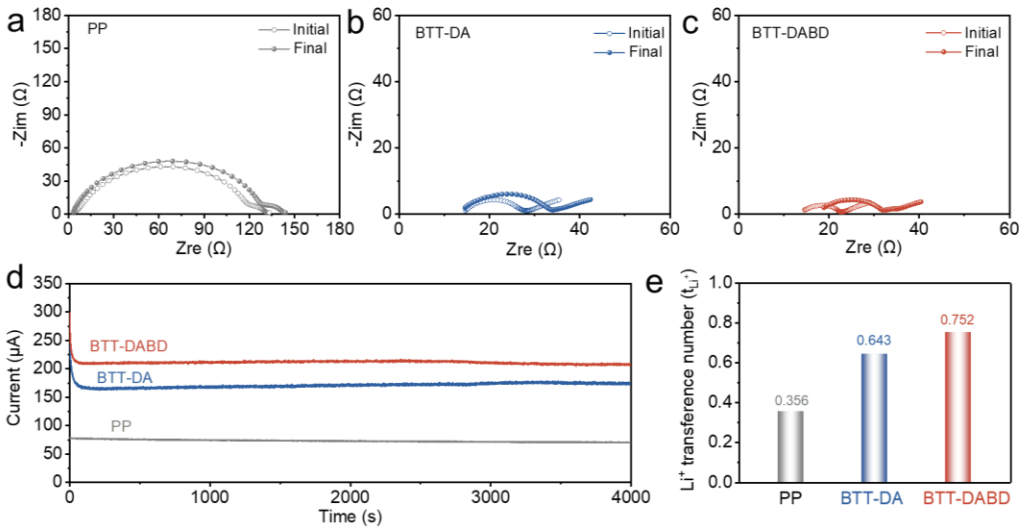

Figure S14. Nyquist plots of the Li||Li symmetric cell with (a) PP, (b) BTT-DA, and (c) BTT-DABD separators before and after polarization. (d) Chronoamperometric curve and (e) Li^+ transference number of different separators.

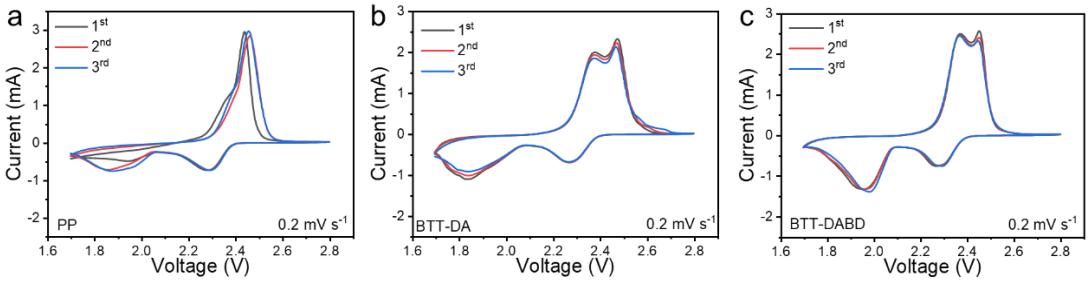

Figure S15. CV curves of Li-S cells with (a) PP, (b) BTT-DA and (c) BTT-DABD separators at 0.2 mV s^{-1}.

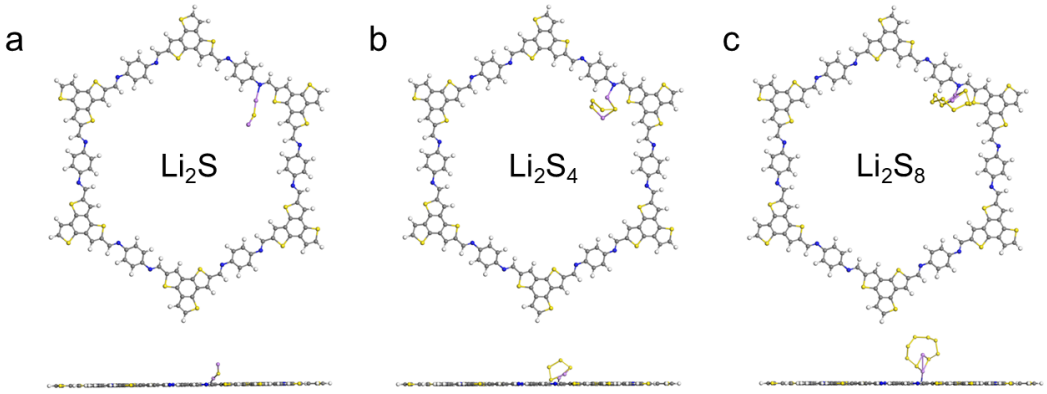

Figure S16. DFT simulated geometrically stable configurations of (a) Li_2S, (b) Li_2S_4, and (c) Li_2S_8 on BTT-DA.

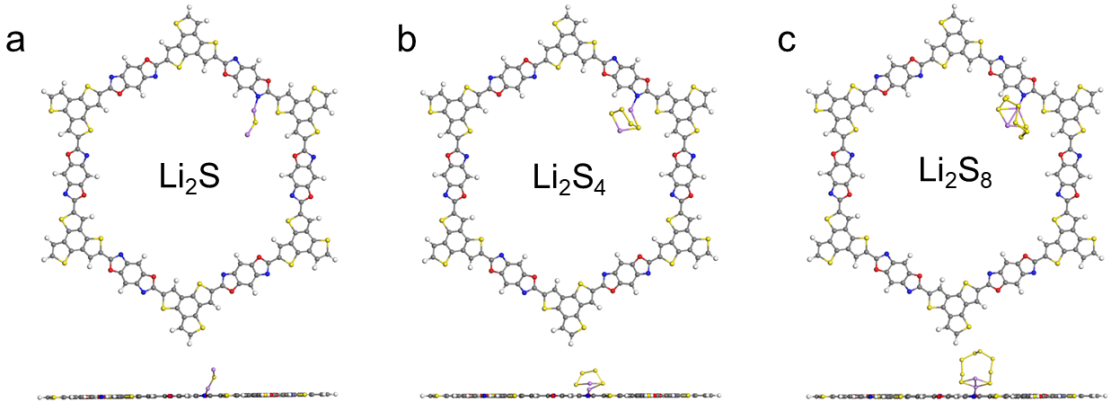

Figure S17. DFT simulated geometrically stable configurations of (a) Li_2S, (b) Li_2S_4, and (c) Li_2S_8 on BTT-DABD.

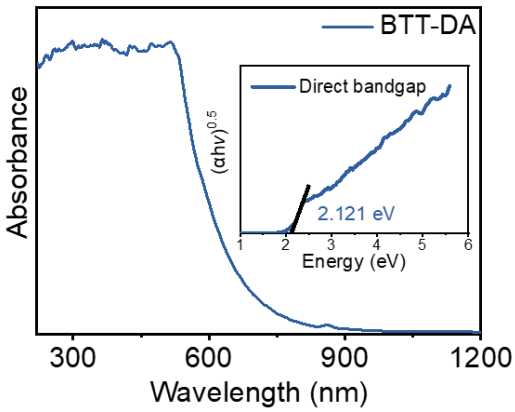

Figure S18. UV/vis absorption spectra and Tauc plots of BTT-DA.

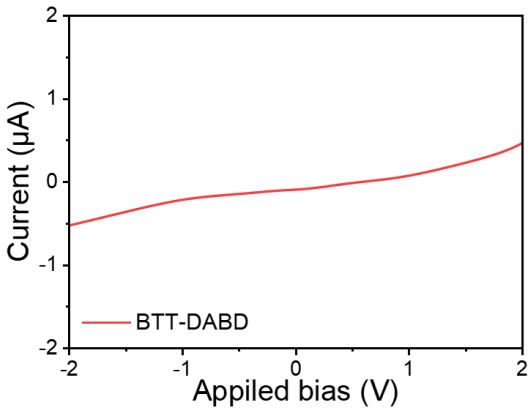

Figure S19. The I-V curve of BTT-DABD at 60 °C. The conductivity of BTT-DA is too low to measure.

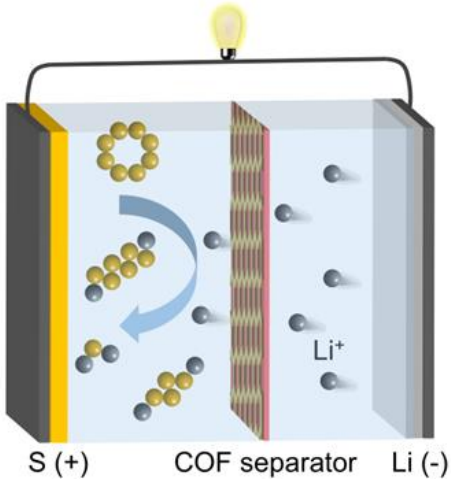

Figure S20. Schematic diagram of the BTT-DABD-involved Li-S battery.

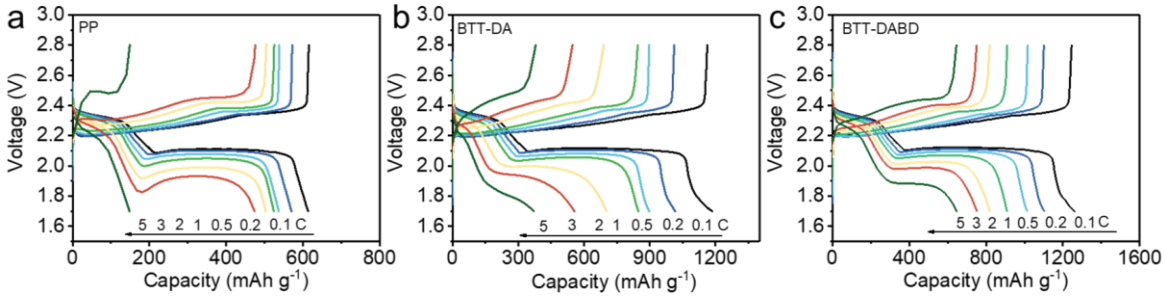

Figure S21. Galvanostatic charge-discharge curves of Li-S cells with (a) PP, (b) BTT-DA, and (c) BTT-DABD separators.

Figure S22. Photographs of cycled Li anodes for (a) PP, (b) BTT-DA, and (c) BTT-DABD separators, respectively.

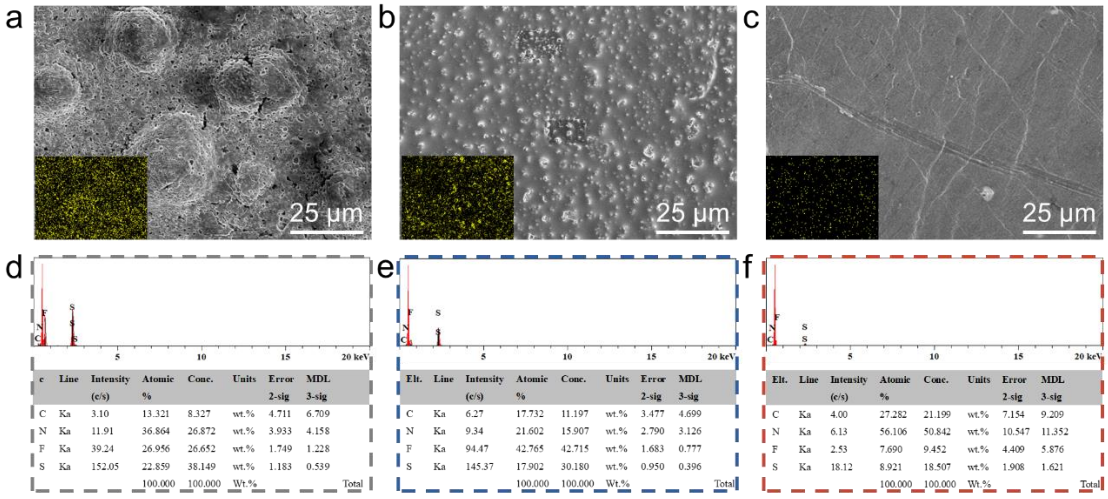

c	Line	Intensity (c/s)	Atomic %	Conc.	Units	Error 2-sig	MDL 3-sig
C	Ka	3.10	13.321	8.327	wt.%	4.711	6.709
N	Ka	11.91	36.864	26.872	wt.%	3.933	4.158
F	Ka	39.24	26.956	26.652	wt.%	1.749	1.228
S	Ka	152.05	22.859	38.149	wt.%	1.183	0.539
			100.000	100.000	Wt.%		Total

Elt.	Line	Intensity (c/s)	Atomic %	Conc.	Units	Error 2-sig	MDL 3-sig
C	Ka	6.27	17.732	11.197	wt.%	3.477	4.699
N	Ka	9.34	21.602	15.907	wt.%	2.790	3.126
F	Ka	94.47	42.765	42.715	wt.%	1.683	0.777
S	Ka	145.37	17.902	30.180	wt.%	0.950	0.396
			100.000	100.000	Wt.%		Total

Elt.	Line	Intensity (c/s)	Atomic %	Conc.	Units	Error 2-sig	MDL 3-sig
C	Ka	4.00	27.282	21.199	wt.%	7.154	9.209
N	Ka	6.13	56.106	50.842	wt.%	10.547	11.352
F	Ka	2.53	7.690	9.452	wt.%	4.409	5.876
S	Ka	18.12	8.921	18.507	wt.%	1.908	1.621
			100.000	100.000	Wt.%		Total

Figure S23. (a-c) Metal-Li anode surface morphology and (d-f) the corresponding EDS results for the cells with PP, BTT-DA, and BTT-DABD after 50 cycles at 0.2 C, respectively.

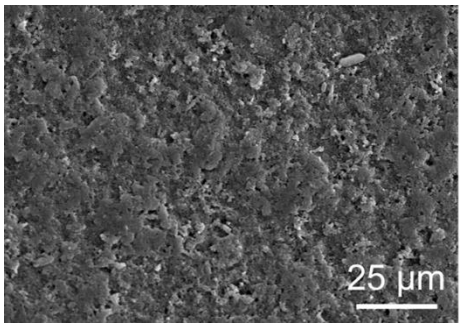

Figure S24. SEM image of the BTT-DABD coating after 50 cycles at 0.2 C.

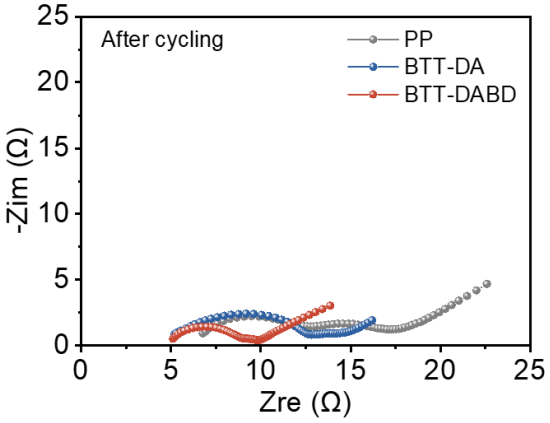

Figure S25. EIS curves of different cells after 50 cycles at 0.2 C.

Table S1. Comparison of the electrochemical performance of the BTT-DABD modified separator with recently-reported COF-based separators and hosts in Li-S cells.

Materials	C-rate	Rate capability (mAh/g)	Cycles	Decay rate per cycle	Ref.
BTT-DABD	5 C	674	500 (3 C)	0.061%	This work
COF-366-OH-IL	2 C	445	300 (1 C)	0.19%	[3]
PyBBT-COF/CNT	3 C	503	500 (1 C)	0.083%	[4]
Zwitterionic COF	4 C	856	500 (2 C)	0.081%	[5]
COF-PDA/SWCNT	5 C	624	500 (1 C)	0.055%	[6]
TpPa-SO_3Li	4 C	633	400 (4 C)	0.039%	[7]
CTF	2 C	802	800 (1 C)	0.052%	[8]
S@TFPB-TAB	4 C	660	400 (1 C)	0.055%	[9]
S@NiS_4-TAPT	4 C	500	400 (2 C)	0.075%	[10]
S–Co@COF-TZ	2 C	667	200 (0.5 C)	0.14%	[11]
COF-ETTA-ETTCA-S	5 C	185	528 (0.5 C)	0.077%	[12]

References

[1] a) G. Kresse, J. Hafner, *Phys. Rev. B* **1993**, *47*, 558; b) G. Kresse, J. Hafner, *Phys. Rev. B* **1994**, *49*, 14251.

[2] a) J. P. Perdew, K. Burke, M. Ernzerhof, *Phys. Rev. Lett.* **1996**, *77*, 3865; b) G. Kresse, D. Joubert, *Phys. Rev. B* **1999**, *59*, 1758; c) P. E. Blöchl, *Phys. Rev. B* **1994**, *50*, 17953.

[3] Y. Zhang, C. Guo, J. Zhou, X. Yao, J. Li, H. Zhuang, Y. Chen, Y. Chen, S.-L. Li, Y.-Q. Lan, *Small* **2023**, *19*, 2206616.

[4] R. Wang, Q. Cai, Y. Zhu, Zh. Mi, W. Weng, Y. Liu, J. Wan, J. Hu, C. Wang, D. Yang, J. Guo, *Chem. Mater.* **2021**, *33*, 3566.

[5] Y. Cao, Y. Zhang, C. Han, S. Liu, S. Zhang, X. Liu, B. Zhang, F. Pan, J. Sun, *ACS Nano* **2023**, *17*, 22632.

[6] L. Han, Y. Yang, S. Sun, J. Yue, J. Li, *Acs Sustain. Chem. Eng.* **2023**, *11*, 8431.

[7] Y. Cao, H. Wu, G. Li, C. Liu, L. Cao, Y. Zhang, W. Bao, H. Wang, Y. Yao, S. Liu, F. Pan, Z. Jiang, J. Sun, *Nano Lett.* **2021**, *21*, 2997.

[8] Q. X. Shi, H. J. Pei, N. You, J. Wu, X. Xiang, Q. Xia, X. L. Xie, S. B. Jin, Y. S. Ye, *Chem. Eng. J.* **2019**, *375*, 121977.

[9] Z. Wang, X. Wu, S. Wei, Y. Xie, C.-Z. Lu, *Chem. Mater.* **2024**, *36*, 2412.

[10] S. Lv, X. Ma, S. Ke, Y. Wang, T. Ma, S. Yuan, Z. Jin, J.-L. Zuo, *J. Am. Chem. Soc.* **2024**, *146*, 9385.

[11] Z. Wu, J. Luo, Y. Liang, X. Yu, Y. Zhao, Y. Li, W. Wang, Z. Sui, X. Tian, Q. Chen, *Mater. Chem. Front.* **2023**, *7*, 1650.

[12] B.-Y. Lu, Z.-Q. Wang, F.-Z. Cui, J.-Y. Li, X.-H. Han, Q.-Y. Qi, D.-L. Ma, G.-F. Jiang, X.-X. Zeng, X. Zhao, *ACS Appl. Mater. Interfaces* **2020**, *12*, 34990.